Changes in the transcriptome of thyroid cancer cell lines after radiotherapy and analysis of the potential mechanisms regulating radiotherapy sensitivity

Yinlong Zhao
Second Affiliated Hospital of Jilin University
Yu Liu
Second Affiliated Hospital of Jilin University
Lili Zhong
Second Affiliated Hospital of Jilin University
Jianfeng Ji
Zhejiang Cancer Hospital
Heqing Yi (yiheqing1980@163.com)
Cancer Hospital of the University of Chinese Academy of Sciences

Research Article

Keywords: Thyroid cancer, radiosensitivity, ceRNA network, lncRNA, circRNA

Posted Date: April 18th, 2022

DOI: https://doi.org/10.21203/rs.3.rs-1550832/v1

Abstract

Background

^{131}Iodine (^{131}I) is an important method for the treatment of thyroid cancer. However, resistance to ^{131}I therapy in some patients results in treatment failure due to the mechanisms involving iodine metabolism and radiotherapy sensitivity. At present, the mechanism of radiosensitivity of ^{131}I treatment for thyroid cancer is not sufficiently documented.

Methods

Time course data on transcriptome differential expression were obtained by next-generation sequencing after administration of high-dose radiation therapy to thyroid cancer cell lines (treated vs. control). Based on the fuzzy clustering algorithm, the time course data were analyzed with the Mfuzz software package, and then the series of clusters reflecting the differential expression trend of the transcriptome was obtained. Bioinformatics was used to construct ceRNA-miRNA-mRNA networks, protein-protein interaction (PPI) networks, survival analysis, and Cox regression analysis to identify competing endogenous RNA (ceRNA) pathways associated with radiosensitivity.

Results

Six time-course clusters with differentiated changing trends are obtained after radiation therapy. Six ceRNA networks are constructed from the 6 time-course clusters transcriptome data, and the hub genes are screened out. After survival analysis and Cox regression analysis, a total of six genes, BNIP3L, TP53INP2, CHAF1A, KDM6B, NUP153, and DCBLD, and their ceRNA pathways were screened. These ceRNA pathways are mainly involved in mitophagy, autophagy, apoptosis, proliferation, DNA damage, and repair, and are closely related to the mechanisms of radio-sensitivity.

Conclusion

We identified several ceRNA pathways potentially involved in the regulation of thyroid cancer radiosensitivity, which provides important clues for the mechanistic study of thyroid cancer radiosensitivity. To our knowledge, this is the first systematic and comprehensive analysis of transcriptome alteration trends in thyroid cancer cells after radiation and the prediction of pathways associated with sensitivity to radiotherapy.

1 Introduction

In 2020, there were 586,202 new cases of thyroid cancer worldwide and 43,646 deaths, accounting for 3.0% and 0.4% of the total number of tumor incidences and deaths, respectively [1]. More than 90% of thyroid cancers are differentiated thyroid cancers (DTC), including papillary thyroid cancer and follicular thyroid cancer. The current treatments for DTC include surgery and postoperative ^{131}I internal

radiotherapy and thyroid hormone suppression therapy. ^{131}I is an effective and safe treatment for patients with unresectable distant metastases and local recurrence after DTC surgery. More than 50% of patients with distant metastases can benefit from ^{131}I therapy [2].

However, patients who are resistant to ^{131}I have a poor prognosis [3]. The cause of ^{131}I resistance is related to dysfunctional iodine metabolism and poor sensitivity to radiotherapy in DTC cells [3, 4]. The regulation of iodine metabolism in DTC involves BRAF gene mutation, TERT promoter mutation, epigenetics, and other mechanisms [5, 6]. Studies have shown that BRAF gene mutations and TERT promoter mutations lead to reduced expression of iodine metabolism genes and reduced ^{131}I uptake in DTC lesions. In particular, when BRAF gene mutations and TERT promoter mutations overlap, thyroid cancer lesions almost lose the ability to take up ^{131}I [5]. The mutation of the BRAR gene reduces the expression of iodine metabolism genes by activating the MAPK pathway [6]. Targeted inhibition of the MAPK pathway can reverse iodine uptake in DTC. It has also been observed that iodine uptake is restored in patients' lesions after treatment by targeting the MAPK pathway [7]. However, studies on the mechanism of radiotherapy sensitivity of ^{131}I in DTC are still limited.

Radiation therapy (x-rays, beta-rays, alpha-rays) deposits energy directly on DNA or indirectly (reactive oxygen species) on DNA, causing DNA damage and initiating the death mechanism [8, 9]. Meanwhile, tumor cells also have some mechanisms, such as DNA damage repair and cell cycle arrest, to avoid cell death induced by DNA damage [8]. ^{131}I serves as a therapeutic agent by emitting beta radiation to induce DNA damage and tumor cell death [10]. Although some patients have an uptake of ^{131}I in their lesions, the treatment is not effective or even progresses, and these patients are radiation therapy-resistant [4, 8]. In this study, thyroid cancer cells were treated with high-dose radiation and total RNA was collected at different times. Through next-generation sequencing and bioinformatics analysis techniques, we screened the characteristic transcriptomic changes in thyroid cancer cells with time progression after radiation therapy and obtained ceRNA pathways that may be associated with radiosensitivity.

2 Method And Materials

2.1 Cell culture

BCPAP cell line was cultured on RPMI-1640 medium (Gibco; ThermoFisher, Shanghai, China), supplemented with 10% FBS (Gibco; ThermoFisher, Shanghai, China), 1% non-essential amino acids (Gibco, Fisher, Shanghai, China), 1% sodium pyruvate (100mM), Solution (Gibco; Fisher, Shanghai, China), 100 U/ml penicillin and 100 g/ml streptomycin. BCPAP cell lines were validated by comparing DNA short tandem repeat data with ATCC, DSMZ, JCRBRIKEN, and EXPASY databases, and no multiple alleles were found in these cell lines. BCPAP cell line was certified by Applied Biomaterials Co., Ltd. (Zhenjiang, China).

BCPAP cells were grown in six-well plates and given 6 Gy irradiation after reaching 70% fusion (Siemens AG; 200 cGy/min). Total RNA was obtained at 2 h, 24 h, 48 h, and 72 h after irradiation. TRIzol reagent

(Invitrogen, Shanghai, China) was used to obtain total RNA from the cell lines according to the manufacturer's protocol. A nanodrop spectrophotometer (nanodrop technology) was used to determine the concentration of total RNA. After next-generation gene sequencing (lc-bio, Hangzhou, China), the different expression profiles of each group of RNAs (including mRNA, lncRNA, and circRNA) were obtained.

2.2 Mfuzz time clustering analysis

Using the Mfuzz package in R language and the fuzzy c-means algorithm, the next-generation sequencing data are grouped into different clusters according to the characteristics of time-course changes [11].

2.3 Construction of a regulatory network of competitive endogenous RNAs (ceRNAs)

Long-stranded RNA (mRNA, lncRNA, and circRNA) clusters data obtained by Mfuzz time clustering analysis were used to predict miRNAs sponged by ceRNAs (lncRNA and circRNA), and miRNAs targeting mRNAs using bioinformatics tools included miRMap [12], miRanda [13], miRDB [14], TargetScan [15], miTarBase [16] and starbase [17]. Thus, miRNAs are the core of bridging lncRNA/circRNA and mRNA, and the bioinformatics tool Cytoscape v3.7 [18] was used to predict and construct the regulatory network of lncRNA/circRNA-miRNA-mRNA for each cluster.

2.4 Protein-protein interaction (PPI) network

The online tool STRING [19] was used to analyze protein-protein interactions (PPI). In this study, confidence (combined score) > 0.4 was chosen as the threshold for protein-protein interactions. Cytoscape v3.7 was used to analyze the topology of PPI relationship networks. From biological networks, it can be seen that most biological networks obey the properties of scale-free networks. Therefore, connectivity analysis in network statistics was used to obtain protein interactions in PPI networks. the core nodes of PPI networks serve as hub genes/proteins [20].

2.5 Survival analysis

The hub genes in the above ceRNA network were analyzed by survival analysis and Cox regression analysis using the TCGA database [21]. Based on the median expression of core genes in the TCGA database, they were divided into high and low expression groups.

2.6 Statistical Analysis

Data are expressed as mean ± SEM. Comparisons between two groups were determined by a two-tailed Student's *t-test*. Statistical analyses were performed with SPSS 22.0 software or R software, as detailed in the corresponding study section. $p < 0.05$ was considered statistically significant.

3 Results

3.1 Time-course changes in gene expression profiles after radiotherapy for thyroid cancer cell line.

BCPAP cells were given 6Gy radiation treatment and total RNA was obtained at different time points (2, 24, 48, 72h) and total RNA was obtained from BCPAP cells that did not receive radiation treatment as a control group. After next-generation gene sequencing, transcriptome differential expression gene profiles were obtained for each group of cells after radiation treatment (treatment vs. control).

Mfuzz was used to perform the cluster analysis based on a fuzzy clustering algorithm on the time course data. In total, we found six clusters with different characteristic trends of gene expression profiles (mRNA, circRNA, lncRNA) as time progressed (Fig. 1). The main features of the gene profile pooled by the six clusters showed a decrease first and an increase later (group 1), a continuous decrease (group 2), an early increase and a later decrease (groups 3, 4, and 6) and a continuous increase (group 5) with the progression of time (Fig. 1).

3 .2 Construction of ceRNA network.

miRNAs are the "bridges" connecting long non-coding RNAs (circRNAs and lncRNAs) exerting regulatory effects on mRNA expression. Bioinformatics tools were used to predict the binding relationships between miRNAs and mRNAs, miRNAs and lncRNAs/circRNAs, and to identify the miRNA relationship pairs corresponding to circRNA/lncRNAs and mRNAs in each cluster. Construction of lncRNA-miRNA-mRNA and circRNA-miRNA-mRNA ceRNA network maps using Cytoscape v3.7 (Fig. 2).

3.3 PPI network analysis.

The genes in the above ceRNA network were selected for protein-protein interaction (PPI) analysis using the online tool STRING. the expression of Cluster2 and cluster5 genes was decreasing and increasing. Therefore, the genes of Cluster2 and cluster5 were combined for PPI analysis, and the other clusters were all carried out for separate PPI analysis. The topology of the PPI relationship network was analyzed with Cytoscape v3.7 to obtain the hub proteins involved in the PPI network (Fig. 3).

3.4 Survival analysis

The survival analysis was demonstrated by combining the clinicopathological characteristics of thyroid cancer (THCA) in the TCGA database and the expression of pivotal genes in the PPI network. Univariate Cox regression analysis showed that six genes (BNIP3L, TP53INP2, CHAF1A, KDM6B, NUP153, DCBLD) were associated with survival in patients with thyroid cancer in clusters 1 to 6 (p□0.05, Figure S1). Among the clinicopathological features, age, disease stage, and T-stage were all associated with patient survival (p□0.05, Figure S1). Among them, patients with high expression of CHAF1A and DCBLD had better survival outcomes (p□0.05, Fig. 4C and E). However, patients with high expression of BNIP3L, TP53INP2, KDM6B, and NUP153 had poor survival outcomes (p□0.05, Fig. 4A, B, D, and F).

In the multivariate Cox regression analysis of the above six genes combined with clinicopathological characteristics separately, there was still a significant correlation between age and patient survival in

each group (p□0.05, Figure S2), but individual genes were not significantly correlated with patient survival (p > 0.05, Figure S2). However, KDM6B and age were associated with patient survival in a multivariate COX regression analysis of the above six genes together and clinicopathological characteristics (p□0.05, Fig. 5). By analyzing the ceRNA network diagram (Fig. 2), we obtained ceRNA pathways associated with BNIP3L, TP53INP2, CHAF1A, KDM6B, NUP153, and DCBLD2 (Table 1).

Table 1
Summary of ceRNA network of survival-related hub genes in Univariate Cox Regression analysis

Cluster	lncRNA/circRNA-miRNA-Gene	Genes main functions
Cluster1	Circ-0000643-miR-582-3p/628-5p-BNIP3L	Mitophagy [22], apoptosis [23]
Cluster1	NEAT1-miR-449b-5p-TP53INP2	Autophagy [24], apoptosis [25]
Cluster2	OHRLOS-miR-519b-3p-CHAF1A	mediate chromatin assembly in DNA replication and DNA repair, anti-apoptosis [26, 27]
Cluster3	Circ-0000426-miR-2115-3p/374b-5p-NUP153	DNA damage and repair, proliferation [28, 29]
Cluster3	Circ-0001461-miR-1287-5p-NUP153	DNA damage and repair, proliferation [28, 29]
Cluster4	circ-0001278-miR-19a/b-3p/miR-130a/b-3p/miR-454-3p/miR-301a/b-3p/miR-4295/miR-519b-3p-DCBLD2	Proliferation, migration, apoptosis [30]
Cluster4	Circ-0001388-miR-197-3p-DCBLD2	Proliferation, migration, apoptosis[30]
Cluster5	circ-0000714-miR-29a/b-3p-KDM6B	dual role in cancer[31]

4 Discussion

The biological behavior of tumors is regulated by genes[32]. Radiotherapy sensitivity studies of ^{131}I internal radiotherapy in thyroid cancer are still limited until now. In contrast, characterizing the changes in gene expression profiles after radiotherapy for thyroid cancer can help provide a clear map for studying the sensitivity of ^{131}I internal radiotherapy for thyroid cancer. Competing endogenous RNAs (ceRNAs) mainly included long noncoding RNA (lncRNA) and circular RNAs (circRNAs), which regulate other RNA transcripts by competing for shared microRNAs (miRNAs)[33]. circRNA/lncRNA is endogenous non-coding RNA with specificity and high conservation in expressed sequence, specifically sponge microRNA (miRNA). miRNA is an endogenous conservative non-coding small RNA, which mainly regulates gene expression by binding to the mRNA 3' untranslated region (3' UTR). Therefore, miRNA is a bridge connecting circRNA/lncRNA and mRNA and is involved in the regulation of cell biological processes.

In this study, by analyzing the high-throughput sequencing data of transcriptome RNA at different time points after high-dose radiation treatment of thyroid cancer cells, a circRNA/lncRNA-miRNA-mRNA ternary interaction network was constructed based on the ceRNA theory, and prognostic analysis was performed.

The transcriptome RNA was divided into 6 clusters based on the trend characteristics of changes in transcriptome RNA during the process of time. The potential ceRNA networks involved in regulating the radiosensitivity of thyroid cancer were screened.

Further, carry out the protein-protein interaction (PPI) analysis of the mRNA in the network, and obtain the hub genes involved in the PPI network. Finally, 6 genes (BNIP3L, TP53INP2, CHAF1A, KDM6B, NUP153, DCBLD2) were associated with the survival of patients with thyroid cancer in Univariate Cox Regression analysis (p□0.05). However, the Multivariate Cox Regression analysis indicates only age and the KDM6B gene were correlated with the overall survival of thyroid patients. Although the other five genes did not show any correlation with the patient's survival analyzed by Multivariate Cox analysis, these genes may still play an important biological role in the tumorigenesis and development of thyroid cancer, especially in radiotherapy sensitivity. According to the current research, the biological functions of the six genes are mainly related to mitophagy, autophagy, apoptosis, proliferation, DNA damage, and repair, etc., which are closely related to the mechanism of radiotherapy sensitivity. To the best of our knowledge, studies on the biological functions of ceRNAs associated with six genes in this study, especially radiotherapy sensitivity, are limited.

Our research shows, that BNIP3L was decreased in early expression and increased in later expression after being subjected to radiotherapy. In our analysis, Circ-0000643 potentially regulates the expression of BNIP3L, but no functional studies of Circ-0000643 have been reported to date. The protein encoded by BNIP3L belongs to the induced apoptosis subfamily within the BCL-2 protein family, interacts with viral and cellular anti-apoptosis proteins, and positive regulation of apoptotic process [23]. In the human small intestine, neuroendocrine tumor GOT1-bearing mice were treated with ^{177}Lu-octreotate, and transcriptome gene expression difference analysis (treated vs. control) was performed at the time point from 1d to 41d, and found BNIP3L showed high expression at 41 days after treatment. The author believes that genes that are elevated in the late stages are to inhibit endogenous apoptosis and assist tumor proliferation [34]. TP53INP2 is an important gene involved in the regulation of autophagy. It can interact with autophagy-membrane autophagy-related protein 8 (Atg8) family proteins (including LC3), which promotes activates autophagy flux [24]. Studies have also shown that TP53INP2 is also involved in regulating tumor cell apoptosis [25]. In Cluster1, lncRNA NEAT1 acts as a ceRNA and potentially regulates the expression of TP53INP2. It has been reported that NEAT1 expression is elevated in thyroid cancer, inhibits apoptosis induced by ^{131}I treatment, and promotes invasion and metastasis of thyroid cancer cells [35, 36].

CHAF1A is the largest subunit of the chromatin assembly factor 1 complex, thought to mediate chromatin assembly in DNA replication and DNA repair [26]. Silencing the expression of CHAF1A will reduce the expression of cyclin D1 and cyclin-dependent kinase 2, resulting in lung cancer cell cycle arrest and inhibition of proliferation [26, 27]. In another study, CHAF1A promotes proliferation and inhibits apoptosis of ovarian epithelial cancer [37]. In our study, the biological function of OHRLOS, a ceRNA that potentially regulates CHAF1A, is no related reports yet.

A recent study has shown that after inhibiting NUP153 in the cell line of thyroid cancer, the expression of mTOR/PI3K/AKT decreased, and cell proliferation was significantly inhibited [29]. NUP153 is considered a target for tumor therapy. In our study, after thyroid cancer cells were given high-dose radiotherapy, the expression level of NUDT16 increased slightly after 2 hours, and then decreased rapidly. The mechanism may be related to early DNA damage repair and cell proliferation inhibition[28]. Circ-0001461 as a potential ceRNA for NUP153 in this study promotes proliferation, migration, and invasion in oral squamous cell carcinoma via the miR-145/TLR4/NF-κB axis [38]. DCBLD2 increased in BCPAP cells after radiation initially but started to decrease after 48 hours. DCBLD2 is shown to inhibit tumors, and it also has an effect of oncogenes, depending on different cancer contexts [30]. The study showed that DCBLD2 in metastatic lung adenocarcinoma cancer cells is much higher than that of adjacent tissues, and DCBLD2 can promote cell migration in vitro [39].

KDM6B shows the dual roles of the tumor suppressor gene and oncogene [31]. For example, in squamous cell carcinoma, where the transcription factor CSL is overexpressed, inhibiting the expression of KDM6B, then promotes proliferation of cells, tumorigenesis, and tumor-related inflammation [40]. At the same time, KDM6B is considered to be one of the cohorts of oxygen-sensitive genes, and it increased under low oxygen concentration, which is correlated with good clinical prognosis in different types of cancer [31]. In this study, the KDM6B gene showed a sustained high expression after high-dose radiotherapy. In our analysis, KDM6B is the only gene associated with patient survival in the multivariate Cox regression analysis. Circular RNA circ-0000714, a potential ceRNA regulating KDN6B expression in our data, was reported to regulate the expression of RAB17, leading to chemoresistance in ovarian cancer[41].

4 Conclusion

The transcriptome gene expression profile showed a series of characteristic changes after high-dose radiotherapy in thyroid cancer cells. We found that it is a complex regulatory network for these changing genes. At last, six genes and the predicted ceRNA pathways mainly involve a series of survival and death mechanisms, which are closely related to the mechanism of radiotherapy sensitivity. For the first time, we have mapped the genetic changes in thyroid cancer cells after radiotherapy, providing clues for studies on the sensitivity of thyroid cancer to radiotherapy. The results in our study are mainly based on the bioinformatics database, therefore, the conclusions need to be verified by further studies.

Declarations

Author Contributions

YL. Z. and Y. L. performed all the experiments. LL. Z. performed the data analysis. JF. J. drafted the manuscript. HQ. Y. conceived and designed the study, contributed to the experiments, and drafted the manuscript. All authors reviewed the manuscript.

Acknowledgments

This work was supported by the National Natural Science Foundation of China (Grant number 81502318, 81902722); Zhejiang Province Natural Science Foundation of China (Grant numbers LY20H180007); and The Medical Health Science and Technology Project of Zhejiang Province (Grant numbers 2022504230/2022PY043, 2019RC022)

Conflicts of interest: none

References

1. Sung H, Ferlay J, Siegel RL, Laversanne M, Soerjomataram I, Jemal A, et al. Global Cancer Statistics 2020: GLOBOCAN Estimates of Incidence and Mortality Worldwide for 36 Cancers in 185 Countries. CA Cancer J Clin 2021;71:209-49.
2. Beslic N, Licina S, Sadija A, and Milardovic R. Incidence of Hypothyreoidism after Radioactive Iodine-I131 Treatment in Dependance of Hyperthyreoidism Etiology and Therapy Dose. Med Arch 2017;71:270-3.
3. Van Nostrand D. Radioiodine Refractory Differentiated Thyroid Cancer: Time to Update the Classifications. Thyroid 2018;28:1083-93.
4. Zhao Y, Zhong L, and Yi H. A review on the mechanism of iodide metabolic dysfunction in differentiated thyroid cancer. Mol Cell Endocrinol 2019;479:71-7.
5. Liu J, Liu R, Shen X, Zhu G, Li B, and Xing M. The Genetic Duet of BRAF V600E and TERT Promoter Mutations Robustly Predicts Loss of Radioiodine Avidity in Recurrent Papillary Thyroid Cancer. J Nucl Med 2020;61:177-82.
6. Cancer Genome Atlas Research N. Integrated genomic characterization of papillary thyroid carcinoma. Cell 2014;159:676-90.
7. Huillard O, Tenenbaum F, Clerc J, Goldwasser F, and Groussin L. Restoring Radioiodine Uptake in BRAF V600E-Mutated Papillary Thyroid Cancer. J Endocr Soc 2017;1:285-7.
8. Gudkov SV, Shilyagina NY, Vodeneev VA, and Zvyagin AV. Targeted Radionuclide Therapy of Human Tumors. Int J Mol Sci 2015;17.
9. Kirsch DG, Diehn M, Kesarwala AH, Maity A, Morgan MA, Schwarz JK, et al. The Future of Radiobiology. J Natl Cancer Inst 2018;110:329-40.
10. Morris ZS, Wang AZ, and Knox SJ. The Radiobiology of Radiopharmaceuticals. Semin Radiat Oncol 2021;31:20-7.
11. Futschik ME and Carlisle B. Noise-robust soft clustering of gene expression time-course data. J Bioinform Comput Biol 2005;3:965-88.
12. Tong Z, Cui Q, Wang J, and Zhou Y. TransmiR v2.0: an updated transcription factor-microRNA regulation database. Nucleic Acids Res 2019;47:D253-D8.
13. Vejnar CE, Blum M, and Zdobnov EM. miRmap web: Comprehensive microRNA target prediction online. Nucleic Acids Res 2013;41:W165-8.

14. John B, Enright AJ, Aravin A, Tuschl T, Sander C, and Marks DS. Human MicroRNA targets. PLoS Biol 2004;2:e363.
15. Wong N and Wang X. miRDB: an online resource for microRNA target prediction and functional annotations. Nucleic Acids Res 2015;43:D146-52.
16. Hsu SD, Lin FM, Wu WY, Liang C, Huang WC, Chan WL, et al. miRTarBase: a database curates experimentally validated microRNA-target interactions. Nucleic Acids Res 2011;39:D163-9.
17. Li JH, Liu S, Zhou H, Qu LH, and Yang JH. starBase v2.0: decoding miRNA-ceRNA, miRNA-ncRNA and protein-RNA interaction networks from large-scale CLIP-Seq data. Nucleic Acids Res 2014;42:D92-7.
18. Shannon P, Markiel A, Ozier O, Baliga NS, Wang JT, Ramage D, et al. Cytoscape: a software environment for integrated models of biomolecular interaction networks. Genome Res 2003;13:2498-504.
19. von Mering C, Huynen M, Jaeggi D, Schmidt S, Bork P, and Snel B. STRING: a database of predicted functional associations between proteins. Nucleic Acids Res 2003;31:258-61.
20. He X and Zhang J. Why do hubs tend to be essential in protein networks? PLoS Genet 2006;2:e88.
21. Posner SF and Baker L. Evaluation and extensions of a structural equation modeling approach to the analysis of survival data. Behav Genet 2000;30:41-50.
22. Marinkovic M and Novak I. A brief overview of BNIP3L/NIX receptor-mediated mitophagy. FEBS Open Bio 2021;11:3230-6.
23. Chen YY, Wang WH, Che L, Lan Y, Zhang LY, Zhan DL, et al. BNIP3L-Dependent Mitophagy Promotes HBx-Induced Cancer Stemness of Hepatocellular Carcinoma Cells via Glycolysis Metabolism Reprogramming. Cancers (Basel) 2020;12.
24. You Z, Xu Y, Wan W, Zhou L, Li J, Zhou T, et al. TP53INP2 contributes to autophagosome formation by promoting LC3-ATG7 interaction. Autophagy 2019;15:1309-21.
25. Ivanova S, Polajnar M, Narbona-Perez AJ, Hernandez-Alvarez MI, Frager P, Slobodnyuk K, et al. Regulation of death receptor signaling by the autophagy protein TP53INP2. EMBO J 2019;38.
26. Liu T, Wei J, Jiang C, Wang C, Zhang X, Du Y, et al. CHAF1A, the largest subunit of the chromatin assembly factor 1 complex, regulates the growth of H1299 human non-small cell lung cancer cells by inducing G0/G1 cell cycle arrest. Exp Ther Med 2017;14:4681-6.
27. Yang C, Sengupta S, Hegde PM, Mitra J, Jiang S, Holey B, et al. Regulation of oxidized base damage repair by chromatin assembly factor 1 subunit A. Nucleic Acids Res 2017;45:739-48.
28. Zhang F, Lou L, Peng B, Song X, Reizes O, Almasan A, et al. Nudix Hydrolase NUDT16 Regulates 53BP1 Protein by Reversing 53BP1 ADP-Ribosylation. Cancer Res 2020;80:999-1010.
29. Ma Y, Yin S, Liu XF, Hu J, Cai N, Zhang XB, et al. Comprehensive Analysis of the Functions and Prognostic Value of RNA-Binding Proteins in Thyroid Cancer. Front Oncol 2021;11:625007.
30. Lagunas-Rangel FA. KDM6B (JMJD3) and its dual role in cancer. Biochimie 2021;184:63-71.
31. Weber C, Zhou Y, Lee JG, Looger LL, Qian G, Ge C, et al. Temperature-dependent sex determination is mediated by pSTAT3 repression of Kdm6b. Science 2020;368:303-6.

32. Hanahan D. Hallmarks of Cancer: New Dimensions. Cancer Discov 2022;12:31-46.
33. Liu Y, Khan S, Li L, Ten Hagen TLM, and Falahati M. Molecular mechanisms of thyroid cancer: A competing endogenous RNA (ceRNA) point of view. Biomed Pharmacother 2022;146:112251.
34. Spetz J, Rudqvist N, Langen B, Parris TZ, Dalmo J, Schuler E, et al. Time-dependent transcriptional response of GOT1 human small intestine neuroendocrine tumor after (177)Lu[Lu]-octreotate therapy. Nucl Med Biol 2018;60:11-8.
35. Liu C, Feng Z, Chen T, Lv J, Liu P, Jia L, et al. Downregulation of NEAT1 reverses the radioactive iodine resistance of papillary thyroid carcinoma cell via miR-101-3p/FN1/PI3K-AKT signaling pathway. Cell Cycle 2019;18:167-203.
36. Sun W, Qin Y, Wang Z, Dong W, He L, Zhang T, et al. The NEAT1_2/miR-491 Axis Modulates Papillary Thyroid Cancer Invasion and Metastasis Through TGM2/NFkappab/FN1 Signaling. Front Oncol 2021;11:610547.
37. Xia D, Yang X, Liu W, Shen F, Pan J, Lin Y, et al. Over-expression of CHAF1A in Epithelial Ovarian Cancer can promote cell proliferation and inhibit cell apoptosis. Biochem Biophys Res Commun 2017;486:191-7.
38. Ai Y, Song J, Wei H, Tang Z, Li X, Lv X, et al. circ_0001461 promotes oral squamous cell carcinoma progression through miR-145/TLR4/NF-kappaB axis. Biochem Biophys Res Commun 2021;566:108-14.
39. Chen X, Lv Y, Xu K, Wang X, Zhao Y, Li J, et al. DCBLD2 Mediates Epithelial-Mesenchymal Transition-Induced Metastasis by Cisplatin in Lung Adenocarcinoma. Cancers (Basel) 2021;13.
40. Guo Y, Xiong Z, and Guo X. Histone demethylase KDM6B regulates human podocyte differentiation in vitro. Biochem J 2019;476:1741-51.
41. Guo M, Li S, Zhao X, Yuan Y, Zhang B, and Guan Y. Knockdown of Circular RNA Hsa_circ_0000714 Can Regulate RAB17 by Sponging miR-370-3p to Reduce Paclitaxel Resistance of Ovarian Cancer Through CDK6/RB Pathway. Onco Targets Ther 2020;13:13211-24.

Figures

Figure 1

Characteristics of time course changes of transcriptome genes in BCPAP cells after 6Gy radiotherapy.

a, the gene expression in Cluster 1 continued to decrease and began to increase at 48 hours; b, the gene expression in Cluster 2 showed a continuous downward trend; c, the gene in Cluster 3 increased at first, and then began to decrease at 2 hours; d, the expression of the Cluster 4 genes increased continuously until 24-48h, then begins to decrease; e, the expression of the Cluster 5 continued to increase; f, the expression of the Cluster 6 genes increased slowly until 24h, then begins to decrease.

Figure 2

The ceRNA network of each cluster genes is constructed by using bioinformatics tools to predict the potential binding miRNA.

a to f, ceRNA networks of clusters 1 to 6 were showed, respectively.

Figure 3

Using STRING and Cytoscape v3.7 to construct PPI networks for all genes in each cluster.

a, c, d and e show the PPI networks of cluster1, 3, 4, 6 genes, respectively. b shows the PPI network of cluster 2 and 5 genes.

Figure 4

The correlation between hub genes and patient prognosis.

a, b, d and f, BNIP3L,TP53INP2, NUP153, KDM6B high expression group patients have poor survival outcomes (p□0.05). c and e, the patients with high expression of CHAF1A and DCBLD2 have better survival outcomes (p□0.05).

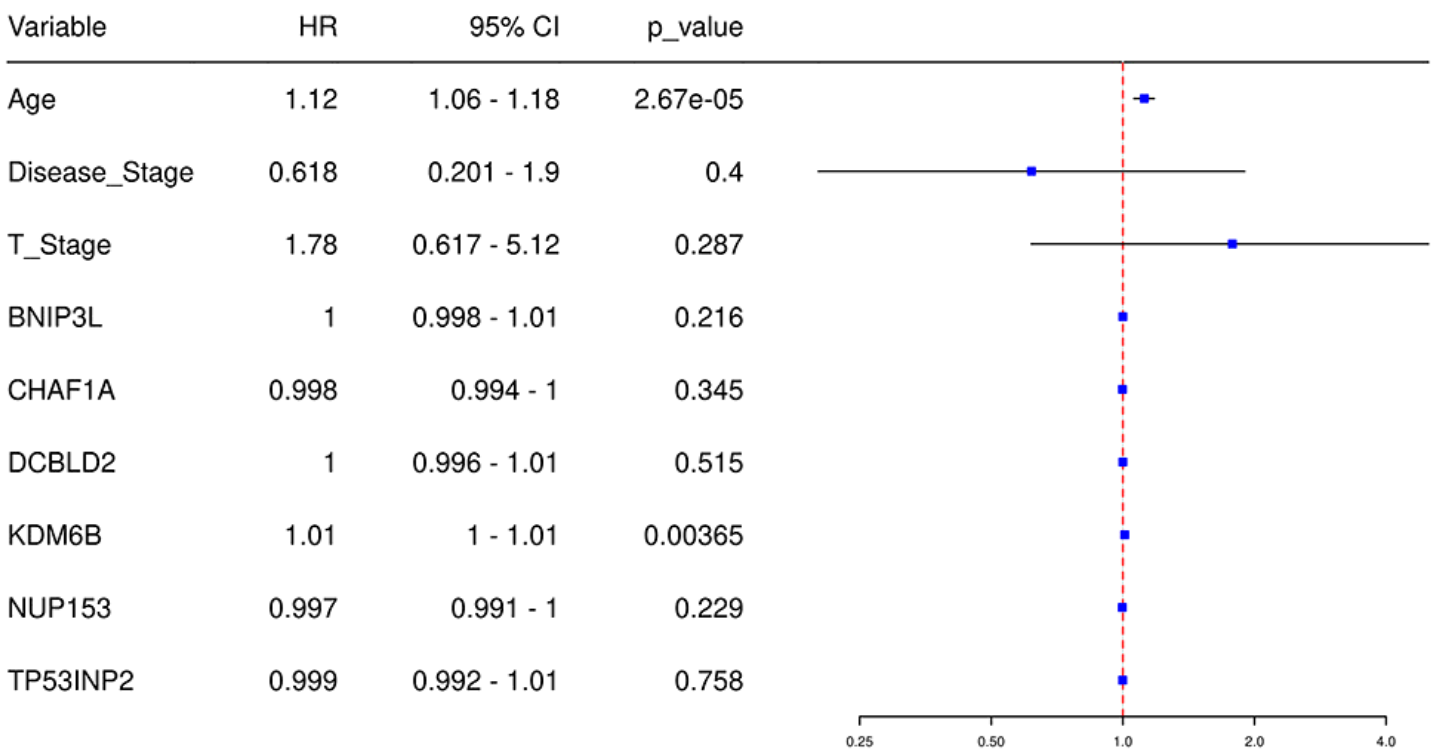

Figure 5

Multivariate Cox regression analysis was used to study the relationship between survival-related hub genes, clinicopathological features and patient survival.

Supplementary Files

This is a list of supplementary files associated with this preprint. Click to download.

- FigureS1.tif
- FigureS2.tif